

*Supporting Information for:*

**Enhanced Ligand Flexibility Accelerates Ligand Substitution Kinetics in Manganese(I)  
Tricarbonyls: Flexible Thianthrene versus Rigid Anthracene Scaffolds**

Jordan Labrecque, Yae-In Cho, Daniel K. McIntosh, Faridat Agboola and Michael J. Rose

*Department of Chemistry, The University of Texas at Austin  
Austin, TX 78757, USA*

<b>Supporting Information Contents</b>	<b>Page</b>
<b>Synthetic Procedures</b>	<b>S2-S4</b>
<b>Ligand Exchange Procedures</b>	<b>S4-S6</b>
<b>NMR spectra</b>	<b>S7-S8</b>
<b>DFT Experimental</b>	<b>S9</b>
<b>X-ray Crystal Structures</b>	<b>S10</b>
<b><math>T_1</math> Relaxation Fits</b>	<b>S11-S12</b>
<b>Substitution reaction IR spectra</b>	<b>S13</b>
<b>Kinetic Plots and table</b>	<b>S14-S16</b>
<b>Dihedral angle scan Plots</b>	<b>S17-S18</b>
<b>X-Ray Crystal Data and Experimental Details</b>	<b>S19-S21</b>
<b>References</b>	<b>S22</b>

## Synthetic Procedures

### Reagents and Physical Methods

All reagents used for the ligand synthesis, metal complexation, and ligand exchange were purchased and used without further purification unless otherwise noted. The synthetic procedures were carried out under inert atmosphere ( $N_2$ ) and dry solvents were purified using a two-column alumina purification system (Pure Process Technology). Deuterated solvents were purchased from Cambridge Isotope Laboratories. The  $^1H$  NMR spectra were collected on an Agilent-Varian DirectDrive MR400 spectrometer with reported chemical shifts referenced to the respective solvent. IR spectra were collected on a Bruker Alpha Fourier transform infrared (FTIR) spectrometer equipped with a diamond ATR crystal. Elemental analysis was performed in duplicate by Midwest Microlab.

**Thianthrene-5-Oxide (Thianth-ox).** Thianthrene (3.00 g, 13.86 mmol) was dissolved in 30 mL of dry DCM and cooled to 0 °C. Separately, *m*CPBA\* (2.87 g, 16.63 mmol) was dissolved in 30 mL of DCM and the solution was cannula transferred to the thianthrene solution, forming a white precipitate. This reaction was stirred at 0 °C for 1 h and washed with 1 M  $NaHCO_3$  (2 × 20 mL), washed with  $H_2O$  (3 × 30 mL), and dried over  $Na_2SO_4$ . The solvent was removed under vacuum to afford a colorless solid as crude product. The product was purified via column chromatography (7:1 Hex:EtOAc) resulting in a colorless powder. Yield: 2.290 g (71%).  $^1H$  NMR ( $CDCl_3$ ,  $\delta$  in ppm): 7.92 (dd 2H), 7.62 (dd 2H), 7.54 (td 2 H), 7.41 (td 2H).

\**Note:* Commercially obtained *m*CPBA contains  $H_2O$  and requires further purification. Approximately 200 mL of  $Et_2O$  was added to 25 g of *m*CPBA which was washed with a buffer solution (410 mL of 0.1 M  $NaOH$  and 250 mL of 0.2 M  $KH_2PO_4$ ). After the wash, the organic layer was dried with  $Na_2SO_4$  and the solvent was removed under vacuum resulting in a colorless, crystalline powder. The dry *m*CPBA was stored in a polypropylene Falcon tube in the freezer. Yield: 15.0 g (60%).

**1,9-Bis(trimethylsilyl)thianthrene Oxide ( $^o=$ Thianth-(TMS) $_2$ ).** Thianth-ox (1.00 g, 4.30 mmol) was dissolved in 30 mL of dry THF. In a separate flask, freshly distilled diisopropylamine (1.52 mL, 10.75 mmol) was added along with 5 mL of dry THF. Both solutions were cooled to -78 °C followed by addition

of *n*BuLi (7 mL, 11.20 mmol) to the diisopropylamine solution to generate the lithiated reagent. The *in situ* generated LDA was then cannula transferred to the **Thianth-ox** solution and allowed to stir at  $-78\text{ }^{\circ}\text{C}$  for 3 h, generating a dark blue solution. The solution was stirred at room temperature for 10 min and then cooled back to  $-78\text{ }^{\circ}\text{C}$  upon which TMS-Cl (1.65 mL, 12.9 mmol) was added via syringe. The reaction slowly warmed to room temperature overnight resulting in a faint yellow solution. Then, 100 mL of  $\text{H}_2\text{O}$  was added to quench the reaction. The mixture was extracted with  $\text{CHCl}_3$  ( $2 \times 40\text{ mL}$ ), washed with  $\text{H}_2\text{O}$  ( $2 \times 100\text{ mL}$ ), and dried over  $\text{Na}_2\text{SO}_4$ . The solvent was removed under vacuum resulting in a white solid dispersed within a yellow oil. Hexanes was used to remove the yellow impurity, ultimately affording a white crystalline material as pure product. Yield: 630 mg (40%).  $^1\text{H NMR}$  ( $\text{CDCl}_3$ ,  $\delta$  in ppm): 7.72 (dd 2H), 7.66 (dd 2H), 7.44 (t 2H), 0.56 (s 18H).

**1,9-Bis(bromo)thianthrene (Thianth-Br<sub>2</sub>).** A 20 mL volume of dry DCM was added to **Thianth-(TMS)<sub>2</sub>** (200 mg, 1.33 mmol). Then,  $\text{Br}_2$  (0.20 mL, 9.31 mmol) was added dropwise via syringe resulting in a dark red-brown solution. The solution was stirred at room temperature for 24 h, avoiding direct light. For simultaneous quenching and deoxygenation, 10 mL of 1 M  $\text{Na}_2\text{SO}_3$  was poured into the solution, that was extracted with DCM ( $3 \times 20\text{ mL}$ ), washed with  $\text{H}_2\text{O}$  ( $2 \times 20\text{ mL}$ ), and dried over  $\text{Na}_2\text{SO}_4$ . The solvent was removed under vacuum affording a white solid as pure product. Yield: 160 mg (80%).  $^1\text{H NMR}$  ( $\text{CDCl}_3$ ,  $\delta$  in ppm): 7.52 (dd 2H), 7.40 (dd 2H), 7.08 (t 2H).

**1,9-Bis(3-pyridine)thianthrene (Thianth-py<sub>2</sub>) (1).** **Thianth-Br<sub>2</sub>** (200 mg, 0.53 mmol),  $\text{Na}_2\text{CO}_3$  (170 mg, 1.60 mmol) and pyridine-3 boronic acid (197 mg, 1.60 mmol) were added to a 50 mL Schlenk flask. Next,  $\text{Pd}(\text{PPh}_3)_4$  (23.1 mg, 4 % mol) was added and the contents were dissolved in dioxane (30 mL). About 5 mL of degassed  $\text{H}_2\text{O}$  was poured into the solution which was then refluxed for 16 h, affording a dark green solution. The product was extracted with EtOAc, washed with  $\text{H}_2\text{O}$  and brine ( $2 \times 30\text{ mL}$  each) and dried over  $\text{Na}_2\text{SO}_4$ . The solvent was removed under vacuum resulting in a dark green oil. Pure product was isolated by column chromatography starting with EtOAc and eluting with DCM/MeOH (5:1) to afford a tan, crystalline solid. Yield: 140 mg (60%).  $^1\text{H NMR}$  ( $\text{CDCl}_3$ ,  $\delta$  in ppm): 8.55 (dd 2H), 8.48 (s 2H), 7.60 (d

2H), 7.50 (d 2H), 7.32 (t 2H), 7.22 (d 2H), 7.15 (t 2H).  $^{13}\text{C}$  NMR ( $\text{CDCl}_3$ ,  $\delta$  in ppm): 149.57, 148.86, 139.16, 137.93, 136.72, 135.49, 134.76, 129.07, 128.84, 127.77, 122.52. X-ray quality colorless prisms were grown via vapor diffusion of pentane into a solution of the ligand in DCM (**Figure S2**).

### Mn Complex Syntheses

**[Mn(Thianth-py<sub>2</sub>)(CO)<sub>3</sub>Br] (3)**. Under N<sub>2</sub> drybox conditions, the **Thianth-py<sub>2</sub>** ligand (22 mg, 0.06 mmol) and Mn(CO)<sub>5</sub>Br (16 mg, 0.06 mmol) were dissolved separately in 5 mL of dry THF. The Mn solution was added dropwise to the ligand solution and allowed to stir at room temperature overnight leading to a turbid yellow solution. The solvent was removed under vacuum resulting in a dark yellow powder. DCM (5 mL) was added to the crude powder and the solution was filtered. The yellow filtrate was reduced under vacuum affording a light yellow solid as product. Yield: 30 mg (85%).  $^1\text{H}$  NMR (MeCN-d<sub>3</sub>,  $\delta$  in ppm): 9.38 (s 1H), 7.88 (d 1H), 7.71 (d 1H), 7.50 (m 4H). Selected IR bands ( $\text{cm}^{-1}$ ): 2018 (vs), 1926 (vs), 1890 (vs), 1593 (w), 1442 (w). Anal. calcd for C<sub>25</sub>H<sub>14</sub>BrMnN<sub>2</sub>O<sub>3</sub>S<sub>2</sub>: C, 50.95; H, 2.39; N, 4.75; found: C, 51.85; H, 2.59; N, 4.40. X-ray quality needles were grown via vapor diffusion of pentane into a solution of the complex in THF (**Figure 1**).

### Ligand Exchange Procedure

**[Mn(Thianth-py<sub>2</sub>)(CO)<sub>3</sub>THF](BF<sub>4</sub>) (5)**. *Note:* This reaction was spectroscopically monitored with infrared spectroscopy and results in a complete conversion. Under N<sub>2</sub> drybox conditions, **3** (20 mg, 0.034 mmol) was dissolved in 3 mL of THF. Subsequently, AgBF<sub>4</sub> (6.60 mg, 0.034 mmol) was added to the solution, resulting in immediate precipitation of a white solid. The solution was stirred for 15 minutes (avoiding direct light), and filtered to afford a yellow solution. Selected IR bands ( $\text{cm}^{-1}$ ): 2045 (vs) 1951 (vs) 1927 (vs).

**[Mn(Thianth-py<sub>2</sub>)(CO)<sub>3</sub>PhCN](BF<sub>4</sub>) (6)**. Under N<sub>2</sub> drybox conditions, two drops of benzonitrile (PhCN) were added to a stirring solution of **5**. The solution was stirred overnight and filtered, and the filtrate was evaporated under vacuum to afford a dark gold powder. Selected IR bands ( $\text{cm}^{-1}$ ): 2150 (vw) 2048 (vs) 1940 (vs).

**Re-formation of [(Thianth-py<sub>2</sub>)Mn(CO)<sub>3</sub>Br] (3).** *Note:* This reaction was spectroscopically (analytically) monitored with infrared spectroscopy and results in a complete conversion of **6** to **3**, (**Figure 4**); thus no yield is reported. Under N<sub>2</sub> drybox conditions, tetraoctylammonium bromide (TOAB) (14.44 mg, 0.026 mmol, 1.2 equiv.) was dissolved in 0.5 mL of THF and **6** (15 mg, 0.022 mmol, 1 equiv) was separately dissolved in 2 mL of THF. The TOAB solution and the solution of **6** were cooled to 0 °C and the TOAB solution was added to the solution of **6** via syringe. The solution was stirred at 0 °C for five min and subsequently warmed to room temperature with no observed color change. Selected IR frequencies (cm<sup>-1</sup>): 2026 (vs) 1938 (vs) 1900 (vs).

*Note:* Tetraoctylammonium bromide was triturated with MeCN and subsequently dried under vacuum and heat (100 °C) overnight before use to remove water.

**[(Anth-py<sub>2</sub>)Mn(CO)<sub>3</sub>THF](BF<sub>4</sub>) (7).** *Note:* This reaction was spectroscopically monitored with infrared spectroscopy and results in a complete conversion. Under N<sub>2</sub> drybox conditions, **4** (20 mg, 0.036 mmol) was dissolved in 3 mL of THF. Subsequently, AgBF<sub>4</sub> (7 mg, 0.036 mmol) added to the solution, resulting in immediate precipitation of a white solid. The solution was stirred for 15 minutes (avoiding direct light), and filtered to afford a yellow solution as product. Selected IR bands (cm<sup>-1</sup>): 2044 (vs) 1939 (vs).

**[(Anth-py<sub>2</sub>)Mn(CO)<sub>3</sub>PhCN](BF<sub>4</sub>) (8).** Under N<sub>2</sub> drybox conditions, two drops of benzonitrile (PhCN) were added to the stirring solution of **7**. The solution was stirred overnight and filtered, and the filtrate was reduced under vacuum to afford a yellow powder. Selected IR bands (cm<sup>-1</sup>): 2155 (vw) 2048 (vs) 1944 (vs).

**Re-formation of [(Anth-py<sub>2</sub>)Mn(CO)<sub>3</sub>Br] (4).** This reaction was spectroscopically (analytically) monitored with infrared spectroscopy and results in a complete conversion of **8** to **4**, (**Figure 4**); thus no yield is reported. Under drybox conditions, tetraoctylammonium bromide (TOAB) (14.44 mg, 0.026 mmol, 1.2 equiv.) was dissolved in 0.5 mL of THF and **8** (14.50 mg, 0.22 mmol, 1 equiv) was separately dissolved in 2 mL of THF. The TOAB solution and the solution of **8** were cooled to 0 °C and the TOAB solution was

added to the solution of **8** via syringe. The solution was stirred at 0 °C for five minutes and subsequently warmed to room temperature with no observed color change. Selected IR frequencies ( $\text{cm}^{-1}$ ): 2026 (vs) 1938 (vs) 1900 (vs).

## NMR Spectra

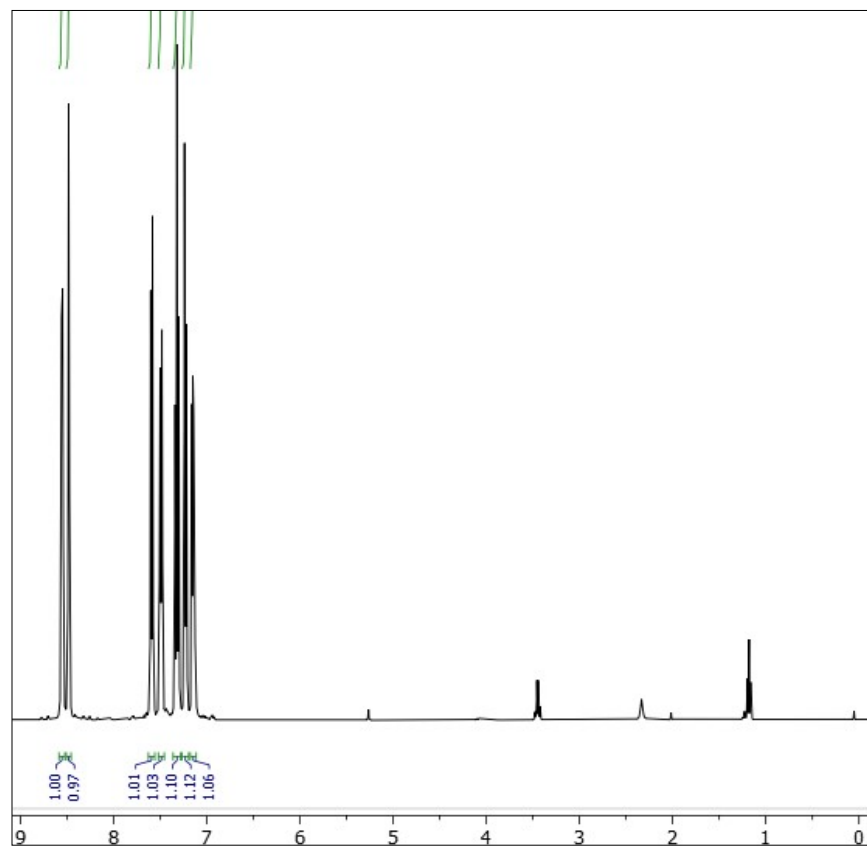


**Figure S1.**  $^1\text{H}$  NMR spectrum of the Thianth-py<sub>2</sub> ligand (**1**) in  $\text{CDCl}_3$ .

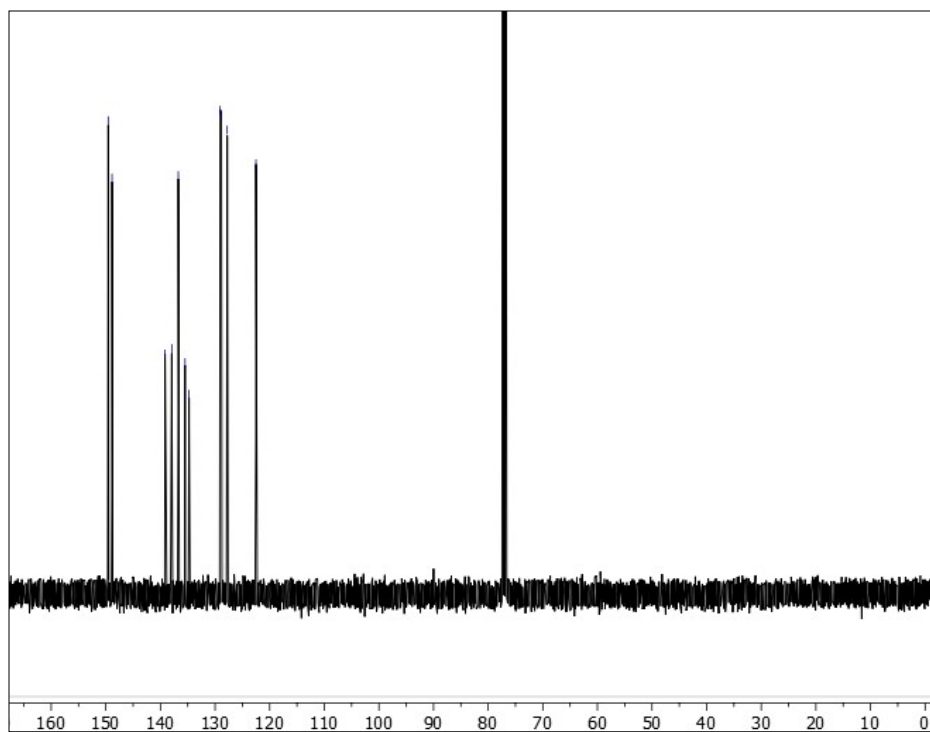


**Figure S2.**  $^{13}\text{C}$  NMR spectrum of the Thianth-py<sub>2</sub> ligand (**1**) in  $\text{CDCl}_3$ .

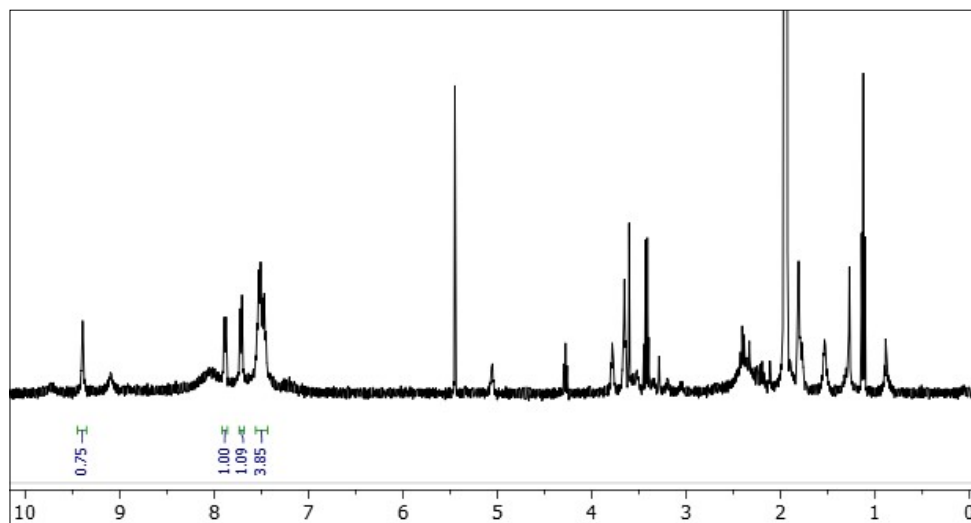


**Figure S3.**  $^1\text{H}$  NMR spectrum of the  $[(\text{Thianth-py}_2)\text{Mn}(\text{CO})_3\text{Br}]$  complex (**3**) in  $\text{MeCN-d}_3$ .



### DFT Scanning Constrained Angle Calculations

The Orca v5.03 program package was used for all geometry optimizations (TZVP basis set for all atoms; BP86 functional). The initial geometry optimizations for **1** and **3** were successfully converged starting from the X-ray coordinates. Proper convergence was subsequently assessed by vibrational analysis to ensure there were no imaginary vibrations prior to the scan. The torsional angle of atoms 1,2,5,4 were constrained to the desired dihedral angle, and the torsional angle of atoms 6,5,2,3 were constrained to the negative of that angle (**Figure S1**). Geometry optimizations were then performed using those constraints. However, while changing the torsional angles successfully elicited the desired motion we sought, they did not directly correspond to the dihedral angle of the scaffold. To calculate this, three carbon atoms were selected from both ‘wings’ of the scaffold to generate two planes and the geometric definition for a dihedral angle was used: inverse cos of the dot product of the norms of the two planes. The dihedral angles were manually calculated in Mercury to ensure accuracy.

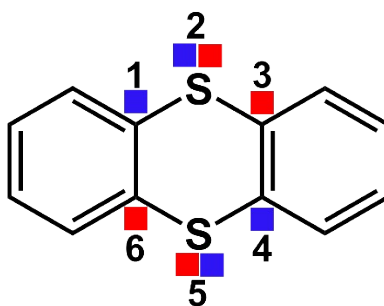


**Figure S4:** Numbering scheme depicting the specific atoms at which the torsion angles were constrained.  
Blue squares: angle 1-2-5-4; red squares: angle 6-5-2-3.

### X-ray Crystal Structures

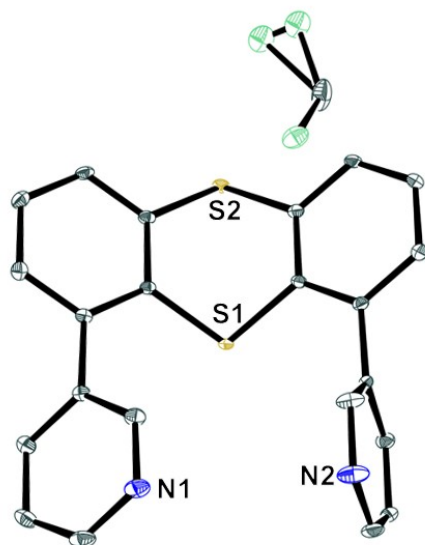


**Figure S5.** ORTEP diagram (30% ellipsoids) depicting the full crystal structure of Thianth-py<sub>2</sub> (**1**); a disordered DCM molecule is in the crystal lattice.

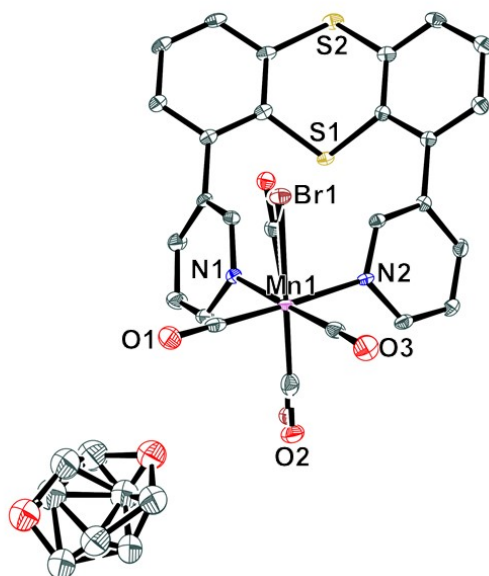


**Figure S6.** ORTEP diagram (30% ellipsoids) depicting the full crystal structure of [(Thianth-py<sub>2</sub>)Mn(CO)<sub>3</sub>Br] (**3**); a disordered THF molecule is in the crystal lattice.

## <sup>1</sup>H NMR $T_1$ Relaxation Fits

*Note:* The <sup>1</sup>H NMR relaxation experiments were performed with Agilent series (400 MHz) spectrometer in CDCl<sub>3</sub> at the same temperature (25 °C) and concentration (15 mM). Prior to measurements, the ligand solutions were degassed with N<sub>2</sub>. Fourteen timepoints were collected following an exponential decay array with the delay ( $d$ ) set to 5 times the longest  $T_1$ . The  $T_1$  data was fit with a three exponential function provided by MestReNova.

## $T_1$ <sup>1</sup>H Relaxation Fits

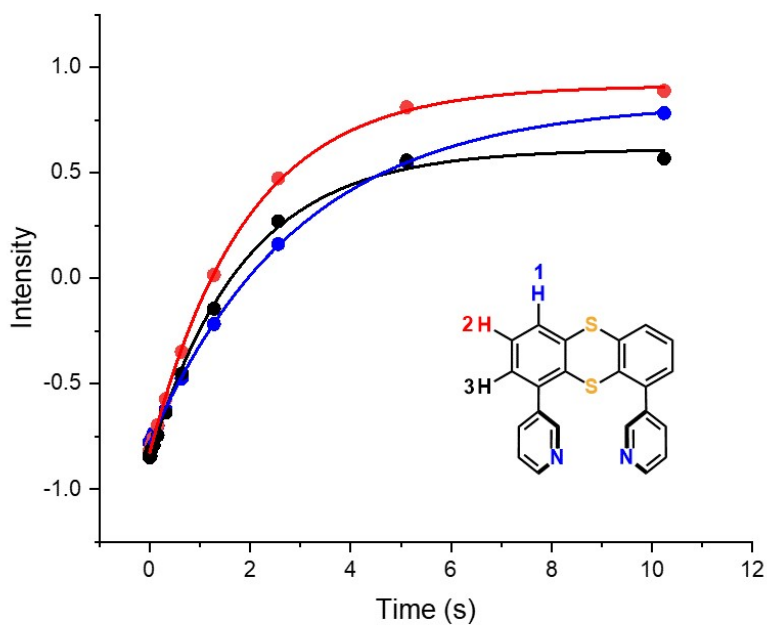


**Figure S7.** Three independent trials of  $T_1$  relaxation fits for the scaffold protons as indicated with a collective error of  $0.44 \pm 0.2\%$ .

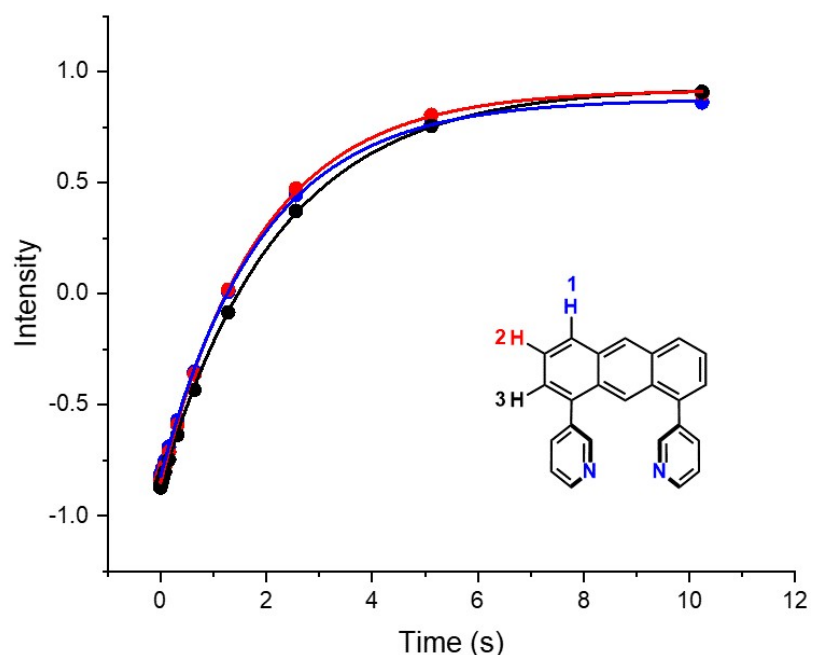


**Figure S8.** Three independent trials of  $T_1$  relaxation fits for the scaffold protons as indicated with a collective error of  $0.36 \pm 0.065\%$ .

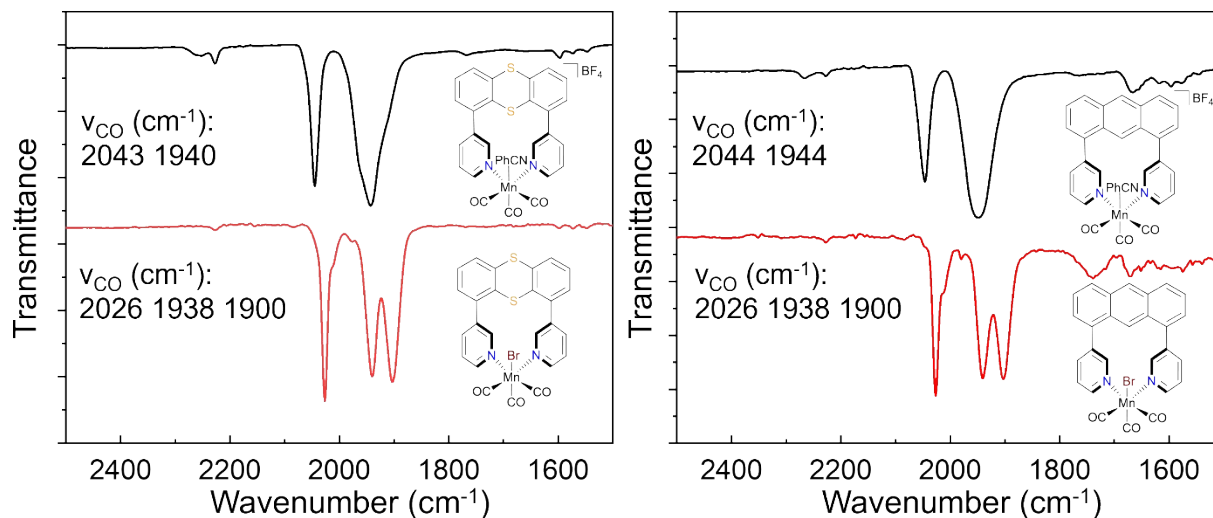


**Figure S9.** IR spectra before (*black trace*) and after (*red trace*) the kinetically monitored ligand exchange reaction (*iii*) for **6** (*left*) and **8** (*right*) with prominent CO stretching frequencies indicated.

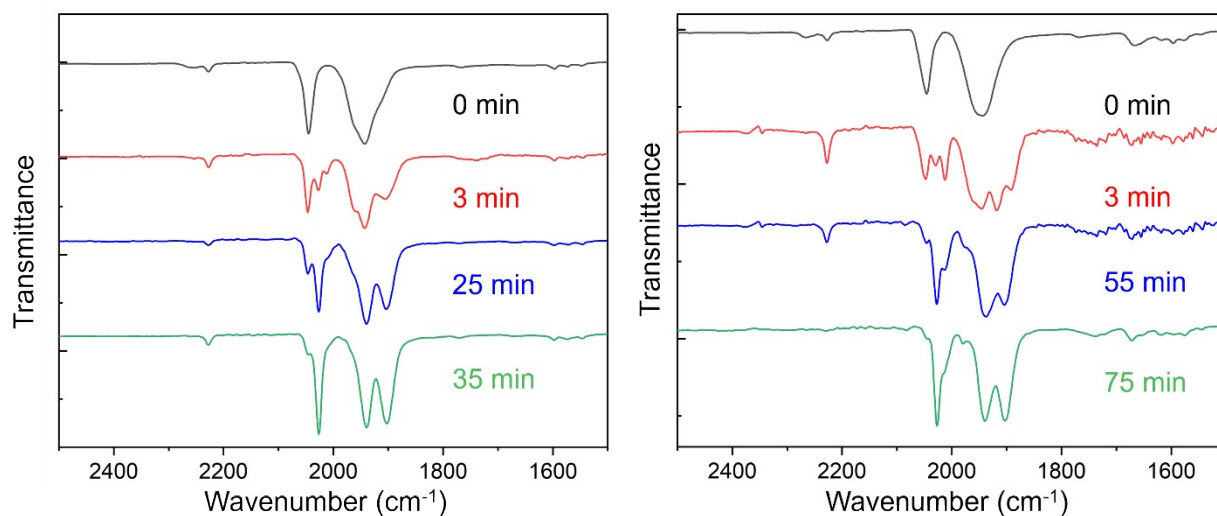


**Figure S10.** Intermediate reaction progress spectra for **6** (*left*) and **8** (*right*).

## Kinetic Plots and Table

\*The data was obtained via a dropcast method and is the average of two ligand exchange reactions. The reaction was initiated at 0 °C and monitored for 15-20 min, and allowed to warm to room temperature to complete the reaction within a reasonable amount of time. Thus, it proved convenient to perform a comparative analysis in the 0 °C and 25 °C regions (holistically shown in ESI, **Figure S7** and **Figure S8**).

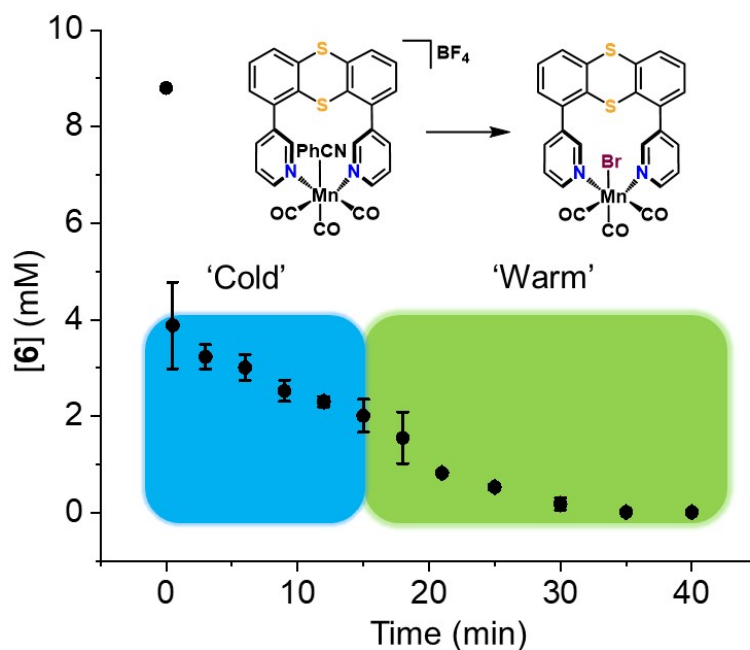


**Figure S11.** Kinetic graph representing the re-formation of **3**. The 'cold' (*blue*) and warm (*green*) regions are highlighted.

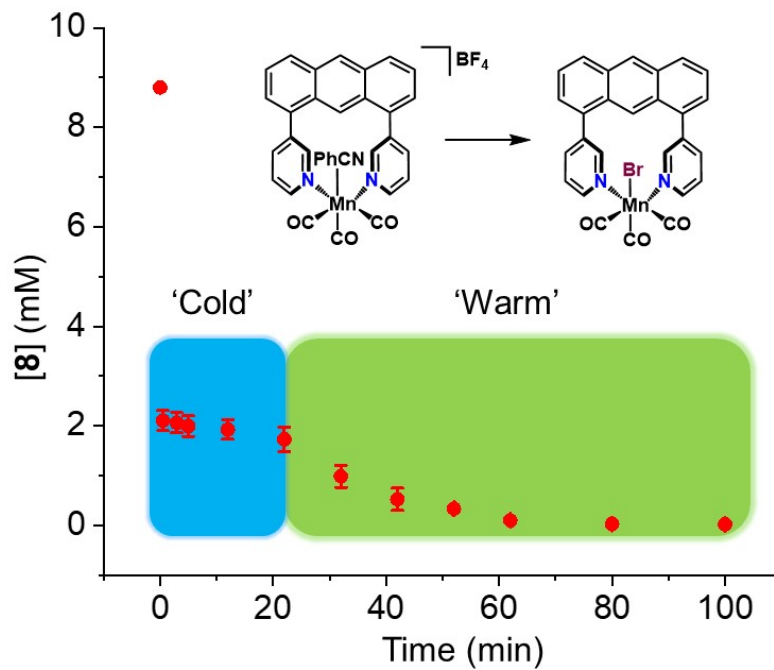


**Figure S12.** Kinetic graph representing the re-formation of **4**. The 'cold' (*blue*) and warm (*green*) regions are highlighted.

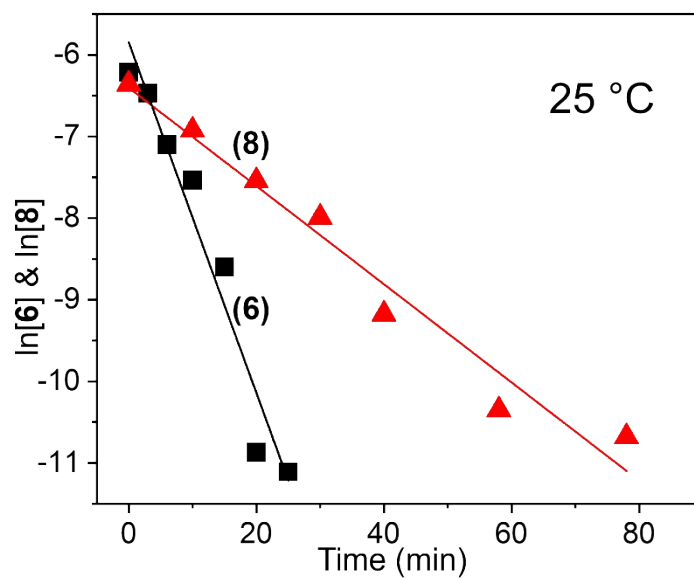


**Figure S13.** Kinetic plot of (iii) at 25 °C. The black squares depict the reaction with **6** (thianthrene scaffold) and the red triangles depict the reaction with **8** (anthracene scaffold).

**Table S1.** Observed rate constants for the formation of **3** and **4** at 25 °C; all data is the average  $\pm$  s.d. of two trials.

Complex	<b>3</b>	<b>4</b>
25 °C $k_{\text{obs}}$ ( $\text{min}^{-1}$ )	$21.74 \times 10^{-2} \pm 0.0342$	$6.01 \times 10^{-2} \pm 0.00523$
25 °C $t_{1/2}$ (min)	$3.19 \pm 0.51$	$11.53 \pm 1.01$

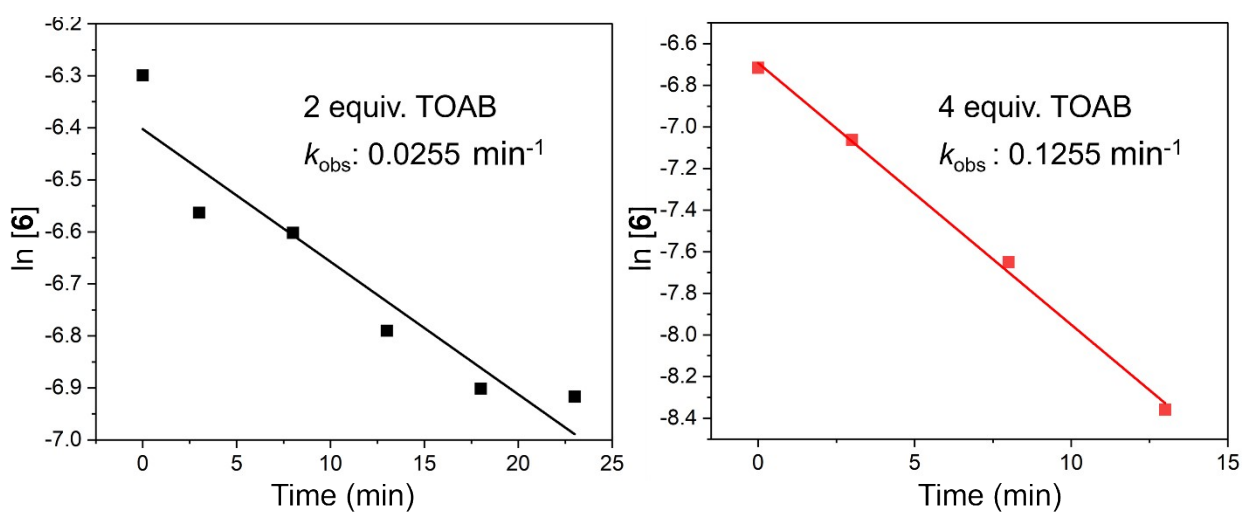


**Figure S14.** Kinetic plots indicating the ligand exchange with **6** at ‘room temperature’ region for two equivalents of TOAB (*left, black squares*) and four equivalents of TOAB (*right, red squares*). (Include the units)



## Dihedral Angle Scan Plots

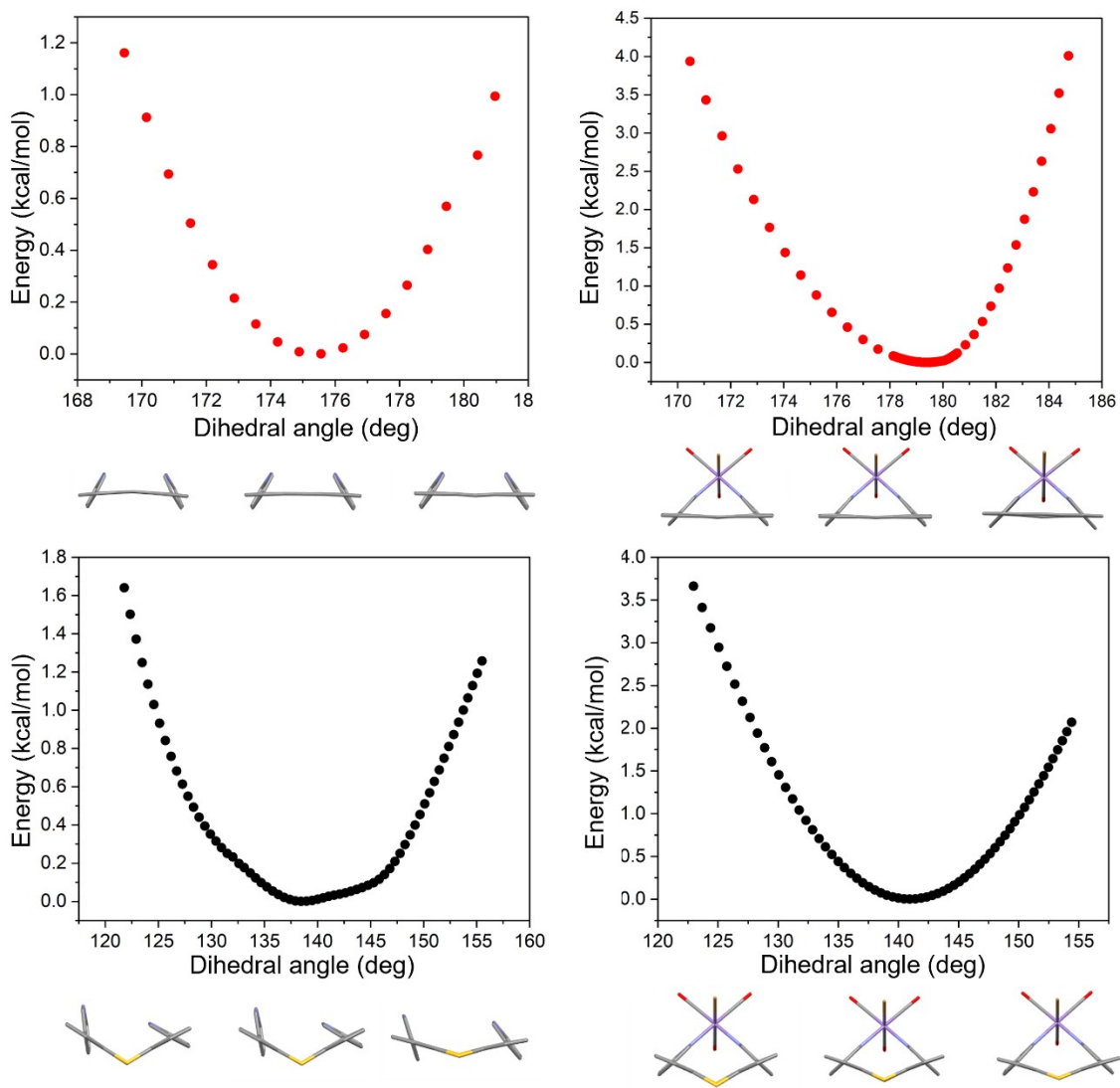


**Figure S15.** Plots of the DFT constrained scaffold angle scan for **2** (top left), **4** (top right), **1** (bottom left), and **3** (bottom right). Selected structures at the extremes and median of the  $kT$  range are depicted beneath the corresponding plots.

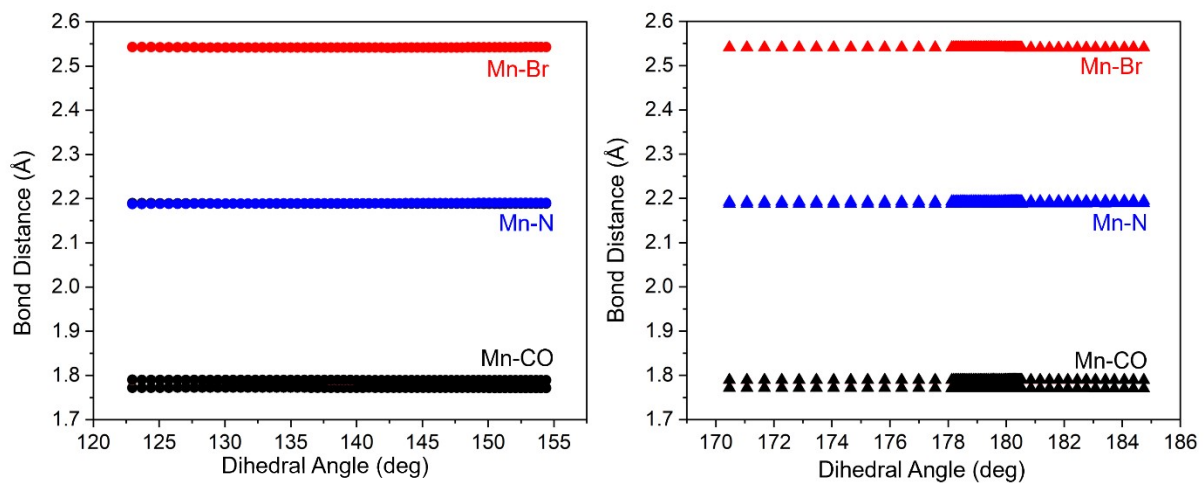


**Figure S16.** Plots of the DFT scaffold dihedral angle scan versus the resulting, invariant M–L bond distances for **3** and **4** (left and right).

### X-ray Crystal Data

	Thianth-py <sub>2</sub> (1)	[(Thian-py <sub>2</sub> )Mn(CO) <sub>3</sub> Br] (3)
Formula	C <sub>23</sub> H <sub>16</sub> N <sub>2</sub> S <sub>2</sub> Cl <sub>2</sub>	C <sub>29</sub> H <sub>22</sub> N <sub>2</sub> O <sub>4</sub> S <sub>2</sub> Br
FW	455.40	661.45
Color	Colorless	Red
Habit	Prism	Prism
Size (mm <sup>3</sup> )	0.39 × 0.22 × 0.16	0.12 × 0.08 × 0.04
T(K)	100	100
Lattice	Triclinic	Triclinic
Space Group	<i>P</i> -1	<i>P</i> -1
a (Å)	7.574(2)	8.798(2)
b (Å)	11.591(3)	9.555(3)
c (Å)	11.938(3)	17.561(4)
α (deg)	77.276(2)	74.444(2)
β (deg)	88.191(2)	80.984(2)
γ (deg)	83.065(2)	76.153(2)
V (Å <sup>3</sup> )	1014.72(5)	1374.22(6)
Z	2	2
d <sub>cal</sub> (g/cm <sup>3</sup> )	1.490	1.599
μ (mm <sup>-1</sup> )	4.897	2.125
GOF on F <sup>2</sup>	1.035	1.132
R indices [ <i>I</i> > 2σ( <i>I</i> )]	R <sub>1</sub> = 0.0486 wR <sub>2</sub> = 0.1384	R <sub>1</sub> = 0.0716, wR <sub>2</sub> = 0.1257
R indices all data	R <sub>1</sub> = 0.0496	R <sub>1</sub> = 0.1048,

	wR <sub>2</sub> = 0.1396	wR <sub>2</sub> = 0.1357
--	--------------------------	--------------------------

### X-Ray Data Collection

**Thianth-py<sub>2</sub> (1):** The data crystal was cut from a larger crystal and had approximate dimensions; 0.39 × 0.22 × 0.16 mm. The data were collected on an Agilent Technologies SuperNova Dual Source diffractometer using a μ-focus Cu Kα radiation source (λ = 1.5418 Å) with collimating mirror monochromators. The data were collected at 100 K using an Oxford 700 Cryostream low temperature device. Data collection, unit cell refinement and data reduction were performed using Rigaku Oxford Diffraction's CrysAlisPro V 1.171.39.46.<sup>1</sup> The structure was solved by direct methods using SHELXT<sup>2</sup> and refined by full-matrix least-squares on F<sup>2</sup> with anisotropic displacement parameters for the non-H atoms using SHELXL-2016/6.<sup>3</sup> Structure analysis was aided by use of the programs PLATON<sup>4</sup> and WinGX.<sup>5</sup> The hydrogen atoms were calculated in ideal positions with isotropic displacement parameters set to 1.2 × U<sub>eq</sub> of the attached atom.

The function,  $\sum w(|F_o|^2 - |F_c|^2)^2$ , was minimized, where  $w = 1/[(\sigma(F_o))^2 + (0.0951 * P)^2 + (2.0615 * P)]$  and  $P = (|F_o|^2 + 2|F_c|^2)/3$ . R<sub>w</sub>(F<sup>2</sup>) refined to 0.1384, with R(F) equal to 0.0486 and a goodness of fit, S, = 1.035. Definitions used for calculating R(F), R<sub>w</sub>(F<sup>2</sup>) and the goodness of fit, S, are given below.<sup>6</sup> The data were checked for secondary extinction effects but no correction was necessary. Neutral atom scattering factors and values used to calculate the linear absorption coefficient are from the International Tables for X-ray Crystallography (1992).<sup>7</sup> All figures were generated using SHELXTL/PC.<sup>8</sup>

**[(Thianth-py<sub>2</sub>)Mn(CO)<sub>3</sub>Br] (3).** The data crystal was cut from a cluster of crystals and had approximate dimensions; 0.12 × 0.08 × 0.04 mm. The data were collected on a Rigaku AFC12 diffractometer with a Saturn 724+ CCD using a graphite monochromator with Mo Kα radiation (λ = 0.71073 Å). The data were collected at 100 K using a Rigaku XStream Cryostream low temperature device. Details of crystal data, data collection and structure refinement are listed in Table S1. Data collection were performed using the Rigaku Americas Corporation's Crystal Clear version 1.40.<sup>1</sup> Unit cell refinement and data reduction were

performed using Agilent Technologies CrysAlisPro V 1.171.39.46.<sup>2</sup> The structure was solved by direct methods using SHELXT<sup>3</sup> and refined by full-matrix least-squares on  $F^2$  with anisotropic displacement parameters for the non-H atoms using SHELXL-2016/6.<sup>4</sup> Structure analysis was aided by use of the programs PLATON<sup>5</sup> and WinGX.<sup>6</sup> The hydrogen atoms on carbon were calculated in ideal positions with isotropic displacement parameters set to  $1.2 \times U_{eq}$  of the attached atom.

The function,  $\sum w(|F_o|^2 - |F_c|^2)^2$ , was minimized, where  $w = 1/[(\sigma(F_o))^2 + (0.0535*P)^2 + (0.4808*P)]$  and  $P = (|F_o|^2 + 2|F_c|^2)/3$ .  $R_w(F^2)$  refined to 0.1257 with  $R(F)$  equal to 0.0716 and a goodness of fit,  $S$ , = 1.130.

. Definitions used for calculating  $R(F)$ ,  $R_w(F^2)$  and the goodness of fit,  $S$ , are given below.<sup>7</sup> The data were checked for secondary extinction effects but no correction was necessary. Neutral atom scattering factors and values used to calculate the linear absorption coefficient are from the International Tables for X-ray Crystallography (1992).<sup>8</sup> All figures were generated using SHELXTL/PC.<sup>9</sup>

## References

- 1) CrysAlisPro. Agilent Technologies (2013). Agilent Technologies UK Ltd., Oxford, UK, SuperNova CCD System, CrysAlisPro Software System, 1.171.39.46.
- 2) SHELXT. Sheldrick, G. M. (2015) *Acta Cryst.* A71, 3-8.
- 3) Sheldrick, G. M. (2015). SHELXL-2016/6. Program for the Refinement of Crystal Structures. *Acta Cryst.*, C71, 9-18.
- 4) Spek, A. L. (2009). PLATON, A Multipurpose Crystallographic Tool. Utrecht University, The Netherlands. *Acta Cryst.* D65, 148-155.
- 5) WinGX 1.64. (1999). An Integrated System of Windows Programs for the Solution, Refinement and Analysis of Single Crystal X-ray Diffraction Data. Farrugia, L. J. *J. Appl. Cryst.* 32. 837-838.
- 6)  $R_w(F^2) = \{\sum w(|F_o|^2 - |F_c|^2)^2 / \sum w(|F_o|^4)\}^{1/2}$  where  $w$  is the weight given each reflection.  
 $R(F) = \sum (|F_o| - |F_c|) / \sum |F_o|$  for reflections with  $F_o > 4(\sum (F_o))$ .  
 $S = [\sum w(|F_o|^2 - |F_c|^2)^2 / (n - p)]^{1/2}$ , where  $n$  is the number of reflections and  $p$  is the number of refined parameters.
- 7) International Tables for X-ray Crystallography (1992). Vol. C, Tables 4.2.6.8 and 6.1.1.4, A. J. C. Wilson, editor, Boston: Kluwer Academic Press.
- 8) Sheldrick, G. M. (1994). SHELXTL/PC (Version 5.03). Siemens Analytical X-ray Instruments, Inc., Madison, Wisconsin, USA.